Biochimica et Biophysica Acta, 1144 (1993) 403–410

BBABIO 43902

Structural characterization of isolated mitochondrial cytochrome c_1

Bih-Show Lou [a], J. David Hobbs [a], Yeong-Renn Chen [b], Linda Yu [b], Chang-An Yu [b] and Mark R. Ondrias [a]

[a] *Department of Chemistry, University of New Mexico, Albuquerque, NM (USA) and* [b] *Department of Biochemistry, Oklahoma State University, Stillwater, OK (USA)*

(Received 8 December 1992)
(Revised manuscript received 21 May 1993)

Key words: Mitochondrion; Respiratory chain; Cytochrome c_1; Heme; Resonance Raman; Active site; (*R. sphaeroides*)

Resonance Raman spectroscopy (RRS) has been employed to characterize cytochromes c_1 isolated from bc_1 complexes of beef heart mitochondria and *Rhodopseudomonas sphaeroides*. The data obtained in this study extend the physical characterization of cytochromes c_1 and focus on the effects of the local protein environment on the heme active site. While the general characteristics of the cytochromes c_1 are similar to those of smaller soluble cytochromes *c*, the behavior of several core-size and ligation-sensitive heme modes reveal that significant systematic differences exist between those species. These, most likely, result from changes in the heme axial-ligand interactions.

Introduction

The major pathway for respiratory electron transport in both photosynthetic bacteria and mitochondria involves a multi-subunit protein complex, cytochrome-*c* reductase (bc_1 complex). Within the past decade, the combined efforts of several laboratories have produced a consistent picture of the subunit structure, general arrangement of redox centers and the overall topology of bc_1 complexes within a membrane. The three or four peptide subunit cytochrome bc_1 complex isolated from photosynthetic bacteria has a relatively simple composition compared with the mitochondrial cytochrome bc_1 complex [1]. Purified mitochondrial cytochrome bc_1 complex has recently been crystallized and found to contain 10 protein subunits [2].

The redox centers of all cytochrome bc_1 complexes consist of two *b*-type cytochromes, one *c*-type cytochrome and one Fe_2S_2 cluster. The cytochromes *b* in the complex exhibit distinct redox and spectroscopic properties. The higher potential heme *b* (approx. +50 mV for bacteria and approx. +90 mV for mitochondria) corresponds to a visible absorption band centered at 562 nm, while the lower potential species (approx. −80 mV for bacteria and approx. −30 mV for mitochondria) exhibits an α-band which is red-shifted by 4–7 nm (depending on the species in question). Cytochrome bc_1 complexes also contain a membrane-bound *c*-type cytochrome c_1 with an E_{m7} in the range +225 to +250 mV in mitochondria and *R. sphaeroides*. Low-temperature EPR data show that all cytochromes in the complexes contain low-spin heme [3]. The iron-sulfur Rieske center in bc_1 complex has an E_{m7} of +280 mV for all systems. A topographical model of bc_1 complex in electron transport membranes [4] places the Rieske FeS protein and cytochrome c_1 subunit on the P-side (cytosolic surface), but has the cytochrome *b* and the core proteins spanning the membrane.

The mitochondrial and bacterial cytochrome bc_1 complexes are functionally analogous. Both catalyze the net oxidation of ubiquinol by soluble cytochrome *c* (mitochrondria) or cytochrome c_2 (bacteria) via a series intracomplex electron transfer reactions. The branched pathways of electron flow within the complex are linked to the oxidation and reduction of pools of bound and free quinones and water-soluble cytochrome *c*. The net energetics of these complex processes have been modeled by the so-called Q [5] and B cycles [6]. These

Correspondence to: M.R. Ondrias, Department of Chemistry, University of Nex Mexico, Albuquerque, NM 87131, USA.

Abbreviations: RR, resonance Raman; RRS, resonance Raman spectroscopy; RDS, Raman difference spectroscopy; CD, circular dichroism; MCD, magnetic circular dichroism; EPR, electron paramagnetic resonance; His, histidine; Met, methionine; Lys, lysine; ATP, adenosine triphosphate; ADP, adenosine diphosphate; E_{m7}, midpoint reduction potential at pH 7.0.

electron transfer cycles are energetically linked to proton translocation across the membrane and the eventual synthesis of ATP from ADP and inorganic phosphate. Cytochrome c_1 in this complex is an indispensable component of the respiratory chain in mitochondria and bacteria. It plays a prominent role in both Q- and B-cycles by transferring an electron from the Fe_2S_2 center to a soluble cytochrome *c*. Therefore, further characterization of the structure and the function of cytochrome c_1 is important for elucidating the mechanisms of electron transport in the cytochrome bc_1 complex.

Resonance Raman spectroscopy (RRS) is a powerful technique for the determination of biostructures and dynamics. RRS is particularly useful for characterizing the local environments of heme protein active sites (most notably heme axial ligation and direct protein/heme interactions). Preliminary studies of bc_1 complexes [7] focused on utilizing selective resonance enhancement for isolating the spectra of the *c* and *b*-type hemes within bacterial (*Rhodospirllium rubrum*) complexes. In this work, we extend our previous studies and focus on heme *c* properties. RRS has been employed to characterize the heme sites of isolated cytochrome c_1, obtained from beef-heart mitochondria and the purple sulfur bacterium, *Rhodopseudomonas sphaeroides*. The spectral properties of isolated cytochrome c_1 subunits were determined and compared to those of soluble cytochrome *c*.

Materials and Methods

Bovine heart cytochrome c_1 [8], cytochrome bc_1 [9] and cytochrome c_1 from *R. sphaeroides* [10] were prepared by previously described methods. Samples were stored in liquid N_2 until needed. Horse heart cytochrome *c* (type V) was obtained from Sigma (St. Louis, MO, USA) and used without further purification. Fully reduced cytochrome c_1 was prepared by degassing solutions of approx. 100 μM protein (in 50 mM phosphate buffer (pH 7.4)) with 4–5 cycles of vacuum/N_2 in an anaerobic optical cell followed by addition of a minimal amount of solid dithionite (Aldrich, Milwaukee, WI, USA) under positive N_2 pressure.

Resonance Raman spectra were obtained with instrumentation described in detail elsewhere [11], which includes a Molectron UV-24 nitrogen-pumped dye laser, a SPEX 1430 double monochromator equipped with an attached water-cooled photomultiplier tube, and a SPEX DM3000R controller. All the spectra were obtained, using approx. 10-ns pulses with spherical focusing optics and average laser power was approx. 5 mW at 15 Hz. Raman shift frequencies were calibrated to well-known bands of benzene.

Spectroscopic measurements with Raman difference spectroscopy (RDS) were carried out using a divided Raman difference cell, and a dual channel Raman spectrometer described elsewhere [12]. The 406.7 nm and 413.1 nm lines from a Krypton ion laser (Coherent) were employed as the exciting source, and the scattered light was collected at 90° to the direction of propagation and polarization of the exciting laser light. The partitioned Raman cell was rotated at 50 Hz. The slits of the spectrometer were adjusted to give 3–4 cm^{-1} resolution. No sample decomposition was observed during acquisition of the spectra.

Results

Absorption spectra

The optical absorption spectra of mitochondrial cytochrome *c* and c_1 (depicted in Fig. 1) are nearly

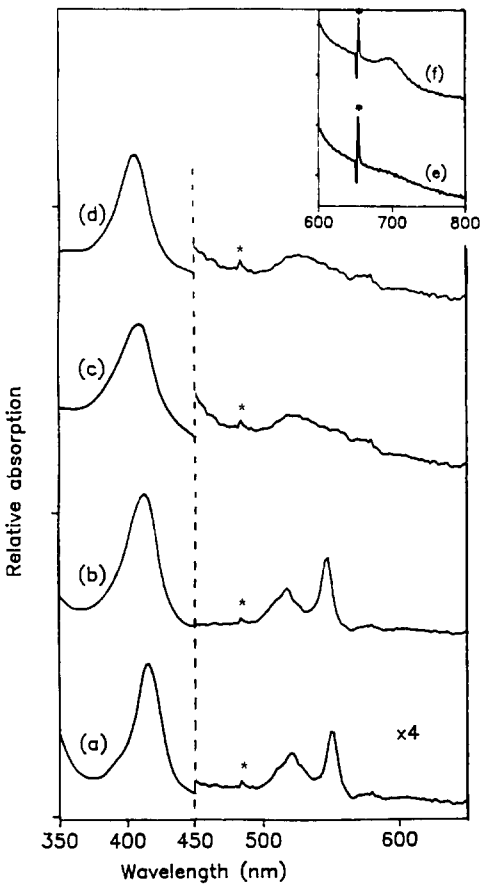

Fig. 1. Optical absorption spectra of (a) fully reduced mitochondrial isolated cytochrome c_1, (b) fully-reduced horse cytochrome *c*, (c) oxidized cytochrome c_1 and (d) oxidized cytochrome *c*. The inset depicts the behavior of 695 nm absorption for oxidized (e) cytochrome c_1 and (f) cytochrome *c*. Reduced samples were prepared by the anaerobic addition of a slight excess of solid sodium dithionite to buffered (50 mM phosphate (pH 7.4)) samples. Oxidized samples were prepared by the addition of a slight excess of potassium ferricyanide to buffered solutions. Excess ferricyanide was removed via gel filtration if necessary. (*) denotes spectrometer artifact.

identical in the B-and Q-band regions for both reduced (Fig. 1a,b) and oxidized forms (Fig. 1c,d). However, the absorbance band at 695 nm (Fig. 1e) observed for ferric cytochrome *c* at neutral pH is much weaker in absorption spectra of mitochondrial cytochrome c_1 (Fig. 1f). This band is characteristic of low-spin cytochromes having methionine as one of the heme axial ligands.

RDS spectra – B-band excitation

Resonance Raman scattering from the heme *b*-band enhances polarized and depolarized heme bands corresponding primarily to in-plane porphyrin ring vibrations. Vibrational modes in the high-frequency region are highly reliable indicators of the heme environment, especially the oxidation and spin-state of the heme. The RR spectra of the oxidized and reduced cytochrome c_1 obtained with B-band excitation are generally similar to those of soluble cytochromes *c* under similar conditions. The positions and relative intensities of the high frequency heme modes are consistent with a low-spin, six-coordinate active site. However, the data obtained by Raman difference spectroscopy (RDS) showed more detailed differences between mitochondrial cytochrome c_1 and cytochrome *c*.

Fig. 2 compares the high-frequency RR spectra for neutral horse heart cytochrome *c* with mitochondrial cytochrome c_1 and alkaline cytochrome *c* in either ferric (Fig. 2-I) or ferrous (Fig. 2-II) forms. The RDS spectra reveal widespread differences between the two cytochromes (*c* and c_1) for both oxidized and reduced species. In general, mitochondrial cytochrome c_1 exhibits a lower frequency in the oxidation-state sensitive mode (ν_4) than cytochrome *c* (at neutral pH), and complicated changes in band positions (summarized in Table I) and intensities in the core-size and ligation-state-sensitive modes (ν_2, ν_3, ν_{10}) are observed.

Comparison of spectra of the ferric proteins reveals small but systematic upshifts of all the bands in the 1500 cm^{-1} to 1650 cm^{-1} region for cytochromes c_1 relative to cytochrome *c*. For example, ν_2, ν_3 and ν_{10} appear at 1586 cm^{-1}, 1504 cm^{-1} and 1636 cm^{-1}, respectively, for cytochrome *c*, but shift to 1588 cm^{-1}, 1505 cm^{-1} and 1640 cm^{-1}, respectively, for cytochrome c_1. The position of ν_4, on the other hand, appears at a slightly lower ($\Delta\nu_4 = 1.1$ cm^{-1}) frequency for cytochrome c_1.

Even larger differences are apparent in RDS spectra of reduced cytochromes c_1 and *c* (Fig. 2-II). The shift in ν_4 to lower frequency for cytochrome c_1 is more pronounced than that exhibited by the oxidized species. The differences in the core-size region between these two cytochromes are quite complicated. Shifts in ν_{10} and ν_3 (to higher frequency) and ν_{11} (to lower frequency) are observed for cytochrome c_1. In addition, the shoulder at 1586 cm^{-1} (ν_{37}) observed for cytochrome *c* is not seen in cytochrome c_1. Instead, bands appear at 1605 cm^{-1} and 1593 cm^{-1}. Finally, the relative intensities of ν_3, ν_{10} and ν_{11} are dramatically decreased in the cytochrome c_1 spectra.

RDS spectra of cytochrome *c* at pH 7.4 and 13.8 were also obtained. Spectra of the ferrous forms of alkaline cytochrome *c* and cytochrome c_1 closely resemble each other, while those of the ferric species differ significantly in the position of ν_4 and the relative intensities of the high-frequency modes.

The isolated mitochondrial ferric cytochrome c_1 displayed a tendency toward photoreduction. This phenomenon was evident in the power-dependent broadening of ν_4 that results from the growth of a reduced ν_4 band (approx. 1360 cm^{-1}, see the inset in Fig. 2-I). In order to eliminate the effects of photoreduction, the RDS spectra shown in Fig. 2-I were obtained in a single scan at low laser power. Although similar photoreduction has been observed in bc_1 complexes, neither cytochrome b_5 nor cytochrome *c* exhibited any photoreduction under similar conditions.

Resonance raman spectra – Q-band excitation

Fig. 3 contrasts the spectra obtained from isolated cytochromes c_1 from *R. sphaeroides* and beef heart mitochondria with those of horse heart cytochrome *c* under neutral and alkaline pH conditions. RR spectra obtained with Q-band excitation are generally dominated by non-totally symmetric vibrational modes effective in mixing the B and Q optical transitions (Herzberg-Teller scattering). These modes are predominantly depolarized. Thus, the polarized modes ν_4 and ν_2 are absent, while ν_{21}, ν_{19}, ν_{11}, and ν_{10} dominate the spectrum.

The RR spectra of heme c_1 obtained with Q-band excitation are also generally similar to those of soluble cytochromes *c*. The strong band at approx. 1313 cm^{-1} in the isolated cytochrome c_1 spectrum is consistent with hemes having thio-ether linkages to the protein via the protoporphyrin vinyl substitute. More detailed comparison to cytochrome *c* reveals specific, systematic differences in the heme c_1 spectra (see Fig. 3a,d).

TABLE I

Some RR modes for equine cytochrome c, mitochondrial cytochrome c_1 and R. sphaeroides cytochrome c_1

	Equine Cyt *c*		Cyt c_1 (mito)		Cyt c_1 (*R. sphaeroides*)	
	III	II	III	II	III	II
ν_4	1374	1364	1374	1362	1372	1362
ν_3	1504	1494	1505	1495	1503	1491
ν_2	1586	1593	1588	1593	1587	1590
ν_{10}	1636	1623	1640	1624		1622
ν_{11}	1563	1547		1543		1540
ν_{19}	1582	1583		1587		1584
ν_{21}		1313		1315		1314

The Q-band RR spectra also reveal small differences between the cytochrome c_1 (Fig. 3c,d) obtained from mammalian mitochondria (beef heart) and photosynthetic bacteria (*R. sphaeroides*). These results are summarized in Table I. The position of ν_{11} and the relative intensities of ν_{11}, ν_{19}, and ν_{10} for both isolated cytochrome c_1 are more similar to those of alkaline cytochrome *c* than cytochrome *c* at neutral pH.

Fig. 3d,e compares the high-frequency RR spectra of mitochondrial reduced isolated cytochrome c_1 and cytochrome bc_1 complex. The scattering observed from the intact bc_1 complex is clearly dominated by heme c_1. The broadening and decreased relative intensities of ν_{11} and ν_{19} in the bc_1 spectrum are attributed to additional contributions to those bands from the *b*-hemes.

Discussion

Recent advances in the isolation and purification of the cytochrome c_1 subunit [10,13] have yielded pure, homogeneous samples that retain their full redox activity. Mitochondrial and bacterial cytochrome c_1 prepared by these methods are quite soluble in aqueous media at neutral pH and allow the properties of a purified component of cytochrome bc_1 complex to be isolated and characterized. Since many properties of horse heart cytochrome *c* are well-known, it serves as a useful point of comparison to the cytochromes c_1.

The present RR studies extend the physical characterization of cytochromes c_1 and focus on the effects of the local protein environment on the structure of the heme active site. Our data confirm that significant

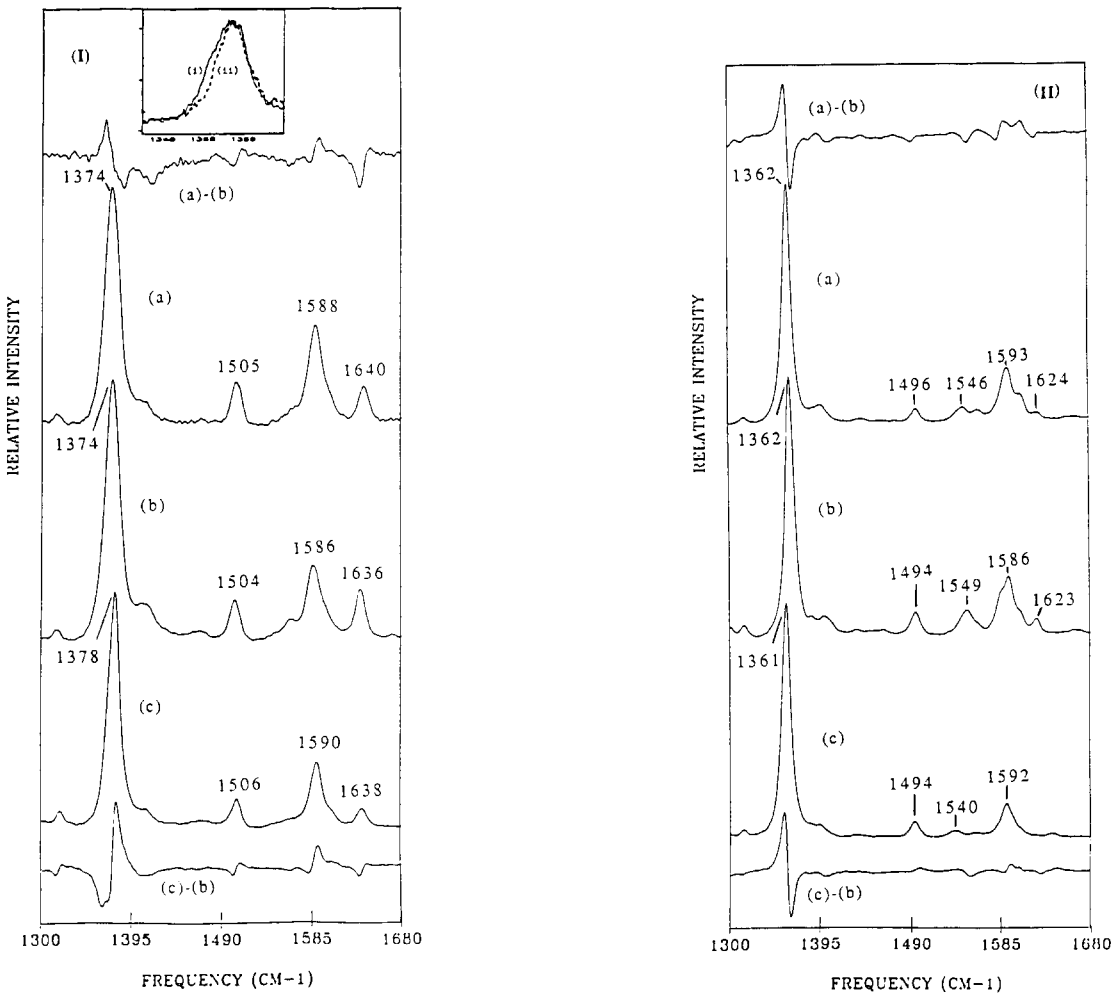

Fig. 2. High-frequency Raman difference spectra of (I) ferric form enzymes: (a) mitochondrial cytochrome c_1, (b) neutral cytochrome *c* (pH 7.4) and (c) alkaline cytochrome *c* (pH 13.8). The top trace shows the difference spectrum of cytochrome c_1 and neutral cytochrome *c* (a − b), and the bottom trace shows the difference spectrum of alkaline and neutral cytochrome *c* (c − b). The excitation wavelength is 406.7 nm. The inset depicts the behavior of ν_4 for ferricyanide oxidized samples under (i) high-power (spherical optics) and (ii) low-power (cylindrical optics) laser excitation. (II) High-frequency Raman difference spectra of ferrous form proteins with excitation wavelength at 413.1 nm. (a) mitochondrial cytochrome c_1, (b) neutral cytochrome *c* (pH 7.4) and (c) alkaline cytochrome *c* (pH 13.8). See text for details.

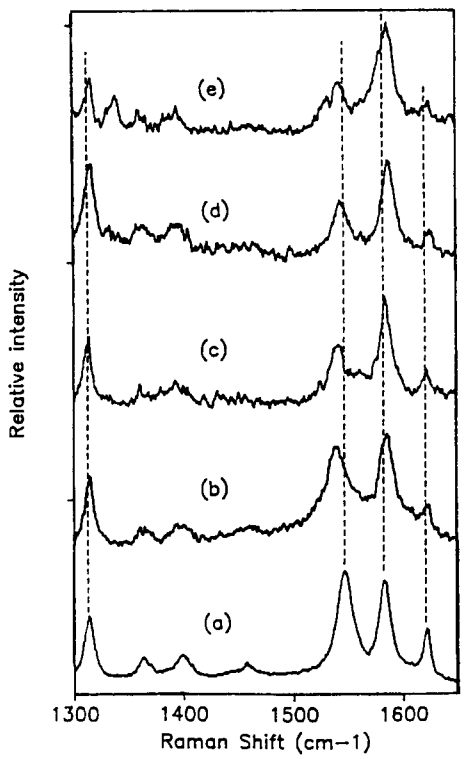

Fig. 3. 550 nm excitation high-frequency RR spectra of reduced (a) neutral horse cytochrome *c* (pH 7.4), (b) alkaline horse cytochrome *c* (pH 13.8), (c) bacterial cytochrome c_1 (pH 7.4), (d) mitochondrial cytochrome c_1 (pH 7.4) and (e) mitochondrial cytochrome bc_1 complex (pH 7.4). Spectra are the unsmoothed sums of 4–6 scans with laser power approx. 5 mW at 15 Hz.

systematic differences exist between the heme sites of cytochromes c_1 and those of smaller soluble cytochromes *c*.

Q-Band RR spectra

The Raman spectrum of ferrous cytochrome c_1 obtained with Q-band excitation is easily distinguished from those of *b*-type cytochromes. Comparison of Fig. 3d and 3e shows that cytochrome c_1 dominates scattering from bc_1 complex at $\lambda = 550$ nm and that the general characteristics of cytochrome c_1 are similar to those of soluble cytochromes *c*. For example, ν_{21} appears as a single band at approx. 1313 cm^{-1} for *c*-type hemes, but is split into two bands by Fermi resonance with a stretching mode of the vinyl substitutes in *b*-type hemes. The positions of core-size marker bands (ν_{10} and ν_{19}) and ν_4 are consistent with a low-spin, six-coordinate heme site (see Table I).

Earlier RDS studies by Shelnutt et al. [12], have demonstrated that heme-active sites of soluble cytochromes *c* are remarkably similar across a wide variety of species. Differences in Raman spectra for any pair of cytochromes *c* are small, confirming that cytochromes *c* from diverse species have very similar heme environments. Systematic differences were detected in the line shape of ν_{21} at 1313 cm^{-1}. These were interpreted to arise from protein conformational changes near cysteine covalent linkages. Our results indicate that the RR spectra of cytochromes c_1 do not fit these patterns. Even though the Q-band RR spectra of isolated cytochrome c_1 are generally similar to those of horse heart cytochrome *c*, systematic differences are evident among the spectra displayed in Fig. 3. These variations strongly suggest that the local protein environment of the heme-active sites in cytochromes c_1 are distinct from those of cytochromes *c*. The largest spectral difference between mitochondrial cytochrome c_1 and horse heart cytochrome *c* occurs in the behavior of ν_{11}. Previous studies by Kitagawa et al. [14], of various *c*-type cytochromes found that ν_{11} is particularly sensitive to the identity and conformation of the heme axial ligands (see Table II). As a general rule, His/Met ligation produces a ν_{11} band that is more intense and at higher frequency ($\geqq 1545$ cm^{-1}) than that exhibited by hemes with two nitrogenous axial ligands. For instance, the ν_{11} band of horse heart cytochrome shift from approx. 1547 cm^{-1} at neutral pH to 1540 cm^{-1} at pH 11.0, concurrent with a change in axial ligation from His/Met to His/Lys.

Qualitatively, the positions and relative intensities of ν_{11} and ν_{19} of mitochondrial and bacterial cytochromes c_1 are more similar to those of alkaline cytochrome *c* or other cytochromes having two nitrogenous axial ligands (Table II). The Q-band RR spectra also reveal small differences between the mitochondrial and bacterial c_1 cytochromes. Clearly, the spectrum of mitochondrial c_1 more closely resembles that of cytochrome *c* at high pH (> 11). We therefore speculate that small but potentially significant structural differences (probably involving the heme axial ligands) also exist between the heme environments of the c_1 cytochromes.

TABLE II

The position of ν_{11} and the 6th ligand on different heme proteins

PP, protoporphyrin.

Cytochrome	ν_{11} (cm^{-1})	Axial ligands
Various soluble Cyt. *c* species (pH 7.0)	1545–1547 [a,b,c]	His/Met
Cyt *c* (pH 11)	1540 [a]	His/Lys
Cyt b_5	1538 [d]	His/His
Cyt *f*	1538 [d]	His/Lys
	1532 [e]	
PP^{2+} (imidazole)	1539 [c]	His/His
PP^{2+} (methylamines)	1530 [c]	His/Lys
Cyt c_1 (mito.)	1543 [a]	His/Met
Cyt c_1 (*R. sphaeroides*)	1540 [a]	His/Met

[a] This work; [b] Ref. 12; [c] Ref. 14; [d] Ref. 7 and [e] Ref. 24.

B-Band spectra

The differences between mitochrondria cytochrome c_1 and horse heart cytochrome *c* were further scruti-

nized by using B-band excitation and Raman Difference Spectroscopy (RDS). Simultaneous acquisition of both cytochrome c_1 and cytochrome c spectra allows for very accurate determination of relative band positions (≤ 0.2 cm^{-1}) and intensities [12]. Because of the qualitative similarity in the Q-band RR spectrum of ferrous mitochondrial c_1 and ferrous cytochrome c at high pH, RDS spectra of cytochrome c at pH 7.4 and pH 13.8 were also obtained. Our data reveal that both mitochondrial cytochrome c_1 and alkaline cytochrome c possess heme environments quite distinct from that of cytochrome c at neutral pH. These produce both the electronic and geometric changes in heme structure reflected in our RDS data.

Spectra of the ferrous forms of mitochondrial cytochrome c_1 and alkaline cytochrome c are very similar, corroborating the results obtained with Q-band excitation. Both differ from the spectrum of cytochrome c at neutral pH in the following ways: (1) ν_4 is shifted to lower frequency by ≥ 1 cm^{-1}; (2) the core-size sensitive modes ν_3 (approx. 1496 cm^{-1}), ν_2 (1593 cm^{-1}), and ν_{10} (1624 cm^{-1}) appear at higher energy (by 1 to 2 cm^{-1}); and (3) bands in the 1540–1580 cm^{-1} region (ν_{11} and ν_2) of the spectrum exhibit large shifts and are significantly reduced in intensity.

The position of ν_4 is a reliable indicator of π^* electron density at the heme [15]. Its behavior in our spectra demonstrates that the heme of cytochrome c at neutral pH has less π^* density than that of the higher pH species. The concerted shifts to higher frequency of the ν_3, ν_2 and ν_{10} convincingly suggest that the heme core size of both mitochondrial cytochrome c_1 and alkaline cytochrome c are contracted relative to cytochrome c at pH 7.4. Finally, the behavior of ν_{11} and ν_{37} confirms the observations made with Q-band excitation and indicates further perturbations in the axial ligation of the heme-active site.

Like their ferrous counterparts, ferric cytochrome c_1 and alkaline cytochrome c exhibit contracted heme cores (i.e., higher frequencies for ν_3, ν_2 and ν_{10}) relative to cytochrome c at pH 7.4. In other respects, however, the spectra of these species are quite distinctive. The difference spectra in Fig. 2-I clearly show that their respective ν_4 bands shift in opposite directions compared to cytochrome c at neutral pH. In addition, the relative intensities of the prominent bands (ν_4, ν_3, ν_2, and ν_{19}) differ substantially. Together, these observations demonstrate that the electronic properties of the heme active site of ferric cytochrome c_1 are distinct from either pH form of cytochrome c.

Heme environments of cytochromes c_1 and c

Isolated mitochondrial cytochrome c_1 and mitochrondrial cytochromes c contain identical prosthetic groups (heme c) that exhibit generally similar optical and redox properties and perform similar electron transfer functions. However, the protein matrices of the cytochromes c_1 differ significantly from those of the soluble cytochromes. Cytochromes c_1 are considerablely larger than their soluble counterparts and while considerable sequence homology exists among bacterial and mitochondrial cytochromes c_1 no significant homology has been found between cytochromes c_1 and cytochromes c. In particular mitochondrial cytochrome c_1 has a higher content of hydrophobic amino acids as commonly found in membranous proteins [16] and its heme group is more deeply buried in the protein matrix than that of cytochrome c [17]. These environmental differences produce little or no effect on the heme visible absorption spectra. The major heme $\pi \rightarrow \pi^*$ transitions for both ferric and ferrous cytochrome c_1 strongly resemble those of cytochrome c. There are, however, clear distinctions in the CD, near-IR, MCD and EPR spectra of mitochondrial cytochromes c_1 relative to cytochromes c [18]. For instance, CD spectra of mammalian cytochromes c_1 exhibit a far UV region typical of a right-handed, α-helical structure [19], but are very different from horse heart cytochrome c in the Soret and α,β-band regions. Optical and magnetic spectra of mitochondrial cytochromes c_1 could be affected by many factors such as the distortion of the heme, the orientation of the porphyrin transition moment, and the geometry and nature of axial ligands [20].

Differences in protein environment apparently have functional manifestations. The redox potential for cytochrome c is 260 mV, but is 228 mV for cytochrome c_1 [10]. Cyanide reacts with mitochondrial ferric cytochrome c and apparently displaces the axial Met-80 ligand, while it is totally unreactive with cytochrome c_1 [21]. Finally, the heme of mitochondrial cytochrome c_1 exhibits a much greater susceptibility to photoreduction under anaerobic conditions than cytochrome c [8].

The resonance Raman spectra obtained in this study further clarify the effects of protein environment on the structure of the heme-active site of cytochromes c_1. The RR bands of cytochrome c_1 have relatively narrow linewidths typical of a homogeneous population of hemes. In addition, the pattern of frequency shifts relative to cytochrome c is not consistent with either systematic distortion of heme planarity (ruffling, doming) or perturbation of the heme peripheral covalent linkages to the protein. We conclude that the heme of cytochromes c_1 occupies a well-defined, homogeneous site that produces little or no steric strain on the macrocycle geometry. We further speculate that the systematic changes (relative to cytochrome c) in the heme electronic state and core size indicated by the high-frequency modes must arise from differences in heme-ligand interactions.

The pH-dependent behavior of cytochromes c pro-

vides a useful model for the effects of ligand exchange on a heme-active site. Ferric horse heart cytochrome *c* undergoes a relatively well-studied transition with a pK_a of approx. 11. This transition is characterized by the loss of the Fe-methionine charge-transfer band at approx. 695 nm and distinctive changes in both the EPR and near-IR MCD spectra of the heme [22]. These changes are consistent with a change in heme axial ligation from the methionine/histidine ligands present at neutral pH. Although His-18 is presumed to remain bound to the heme, the identity of the sixth ligand in alkaline cytochrome *c* has been controversial [22,23]. Recent MCD data indicate that lysine may serve as the sixth ligand, making alkaline cytochrome *c* similar to cytochrome *f* in its ligand configuration [18]. The RR spectra of cytochrome *c* clearly show the effects of ligand exchange. Replacement of methionine with an σ-binding ligand alters the π^* electron density of the heme. In ferrous cytochrome *c*, increased σ donation raises π^* density, lowering the frequency of ν_4. Interestingly, the heme core size (as reflected by the positions of ν_3 and ν_2) is unaffected. In contrast, the heme in ferric cytochrome *c* is evidently quite responsive to the π-backbonding interactions with the methionine ligand. Replacement of methionine produces a decrease in heme π^* electron density (i.e., an increase in ν_4 frequency) and a concomitant decrease in heme core size. The close correspondence of the RR spectra of ferrous mitochondrial cytochrome c_1 and alkaline cytochrome *c*, together with the absence of the Fe-methionine charge transfer band in ferric cytochrome c_1 absorption spectrum suggests, at first blush, that perhaps a simple exchange of methionine for a nitrogenous ligand might be responsible for the properties of the heme site of cytochrome c_1. However, the spectroscopic properties of ferric cytochrome c_1 and evidence from mutagenesis studies (see below) are inconsistent with this scenario.

There are several clear indications that the heme electronic state in mitochondrial ferric cytochrome c_1 differs significantly from that of alkaline cytochrome *c*. For instance, Plamer and co-workers have demonstrated that, while the EPR spectrum of mitochondrial cytochrome c_1 resembles that of alkaline cytochrome *c*, its near-IR MCD spectrum is quite similar to cytochrome *c* at neutral pH [18]. Our data reveal small but significant differences between the hemes of ferric cytochrome c_1 and cytochrome *c* at neutral pH. In fact, the ν_4 bands of cytochrome c_1 and alkaline cytochrome *c* shift in the opposite directions relative to neutral cytochrome *c*. Thus, it is unlikely that simple ligand replacement (His or Lys for Met) is responsible for the structural and functional differences between the heme sites of cytochromes *c* and cytochrome c_1.

Recent, site-directed mutagenesis studies by Gray et al. [25] have demonstrated that Met-183 is the most likely sixth ligand of the cytochrome c_1 isolated from *Rhodobacter capsulatus*. They replaced either of the two conserved methionines (183 and 205) with non-ligating residues. The CM183L mutant did not grow photosynthetically and produce cytochrome c_1 with a dramatically altered mid-point potential. In view of the physical and spectroscopic similarities of bacterial and mitochondrial cytochromes c_1, we assume that the mitochondrial species also possesses His/Met axial ligation.

We conclude that, while it is likely that methionine is the sixth ligand of cytochrome c_1, its orientation relative to the heme is quite different from the axial ligation geometry of neutral cytochromes *c*. This diminishes the Fe-methionine charge transfer interactions and affects the heme structure as evidenced by the behavior of both core size (ν_2, ν_3 and ν_{10}) and axial-ligation (ν_{11}) sensitive vibrational modes. Moreover, these effects are more apparent in the ferrous form of the protein. The combination of electronic and structural perturbations may, in turn, play a major role in regulating the redox potential of the active site.

Acknowledgements

This work was performed at the University of New Mexico and was supported by the National Institutes of Health (GM 33330 to M.R.O. and GM 30721 to C.-A.Y.). The authors thank Drs. Kevin Gray and David Knaff for stimulating discussions.

References

1 Gabellini, N. (1988) J. Bioenerg. Biomembr. 20, 59–82.
2 Yue, W.-H., Zan, Y.-P., Yu, L. and Yu, C.-A. (1991) Biochemistry 30, 2303–2306.
3 Rich, P.R. (1984) Biochim. Biophys. Acta 768, 53–79.
4 Gonzalez-Halphen, D., Lindorfer, M.A. and Capaldi, R.A. (1988) Biochemistry 27, 7021–7031.
5 Mitchel, P. (1976) J. Theor. Biol. 62, 327–367.
6 Wikstrom, M., Krab, K. and Saraste, M. (1981) Annu. Rev. Biochem. 50, 623–655.
7 Hobbs, D.J., Kriauciunas, A., Guner, S., Knaff, D.B. and Ondrias, M.R. (1990), Biochim. Biophys. Acta 1018, 47–54.
8 Yu, C.-A., Chiang, Y.-L., Yu, L. and King, T.E. (1975) J. Biol. Chem. 250, 6218–6221.
9 Yu, C.-A. and Yu, L. (1980), Biochim. Biophys. Acta. 591, 409–420.
10 Yu, L., Dong, J.-H. and Yu, C.-A. (1986) Biochim. Biophys. Acta 852, 203–211.
11 Larsen, R.W. (1990) Ph.D. thesis, University of New Mexico.
12 Shelnutt, J.A., Rousseau, D.L., Dethmers, J.K. and Margoliash, E. (1981) Biochemistry 20, 6485–6497.
13 Yu, C.-A., Yu, L. and King, T.E. (1972) J. Biol. Chem. 247, 1012–1019.
14 Kitagawa, T., Kyogoku, Y., Iizuka, T., Ikeda-Saito, M. and Yamanaka, T. (1975) J. Biochem. 78, 719–728.
15 Spiro, T.G. and Li, X.-Y. (1988) in Biological Applications of Raman Spectroscopy, Vol. 3 (Spiro, T.G., ed.), pp. 67–94, Wiley, New York.

16 Wakabayashi, S., Matsubara, H., Kim, C.H., Kawai, K. and King, T.E. (1980) Biochem. Biophys. Res. Commun. 97, 1548–1554.
17 Kaminsky, L.S., Chiang, Y.-L., Yu, C.-A. and King, T.S. (1974) Biochem. Biophys. Res. Commun. 59, 688–692.
18 Simpkin, D., Palmer, G., Devlin F.J., Mckenna, M.C., Jensen, G.M. and Stephens, P.J. (1989) Biochemistry 28, 8033–8038.
19 Yu, C.-A., Yong, F.C. and King, T.E. (1971) Biochem. Biophys. Res. Commun. 45, 508–513.
20 Myer, Y.P. (1985) Curr. Top. Bioenerg. 14, 149–188.
21 Kaminsky, L.S., Chiang, Y. and King, T.E. (1975) J. Biol. Chem. 250, 7280–7287.
22 Gadsby, P.A., Peterson, J., Foote, N., Greenwood, C. and Thomson, A.J. (1987) Biochem. J. 246, 43–54.
23 Bosshard, H.R. (1981) J. Mol. Biol. 153, 1125–1149.
24 Davis, D.J., Frame, M.K. and Johnson, D.A. (1988) Biochim. Biophys. Acta 936, 61–66.
25 Gray, K.A. Davidson, E. and Daldal, F. (1992) Biochemistry 31, 11864–11873.